Published in: Chemical Physics (2001), vol. 272, pp. 277-292
Status: Postprint (Author's version)

The vacuum UV photoabsorption spectrum of methyl chloride (CH_3Cl) and its perdeuterated isotopomer CD_3Cl II. A vibrational analysis

R. Locht [a,*], B. Leyh [a,1] A. Hoxha [a], D. Dehareng [b], H.W. Jochims [c], H. Baumgärtel [c]

[a] *Département de Chimie Générale et de Chimie Physique, Institut de Chimie, Bât.B6c, Université de Liège, Sart-Tilman par B-4000 Liège 1, Belgium*
[b] *Centre d'Ingéniérie des Protéines, Institut de Chimie, Bât.B6a, Université de Liège, Sart-Tilman par B-4000 Liège 1, Belgium*
[c] *Institut für Physikalische und Theoretische Chemie, Freie Universität Berlin, Takustraße 3, D-14195 Berlin, Germany*

Abstract

The fine structure of the vacuum UV photoabsorption spectrum of CH_3C1 and CD_3C1 has been analyzed in the 7.5-10.5 eV photon energy range. A large number of lines have been observed, classified and assigned to the vibrational excitation accompanying a series of Rydberg transitions. The vibronic transitions involve both Jahn-Teller distortion and spin-orbit splitting. The former effect has been evaluated by ab initio calculations showing that the ^2E state (in the C_{3v} symmetry group) splits into $^2A'$ and $^2A''$ states in the C_s symmetry group. The $^2A'$ state is energetically the lowest component whereas the $^2A''$ is found to be a transition state. The Jahn-Teller stabilization energy and the wave numbers associated with all vibrational modes have been calculated. Experimentally, the entire fine structure could be described by using three vibrational modes, i.e. $hc\omega_5$ = 104 ± 7 meV, $hc\omega_6$ = 77 ± 7 meV and $hc\omega$ = 162 ± 3 meV respectively, as resulting from an average over all the analyzed Rydberg states. In CD_3C1 the corresponding energies are $hc\omega_5$ = 81 ± 4 meV, $hc\omega_6$ = 66 ± *5* meV and $hc\omega$ = 124 ± 4 meV. These values are in good agreement with those predicted by the present ab initio calculations for the the ion ground state. However, the agreement is not so good for the wave number ω which could be assigned to the ν_3 or to the ν_4 vibrational modes. Though some arguments favour ν_4 (the CH_3 umbrella mode), within the error limits on the present measurements it is formally not possible to ascribe this wave number to one of these two vibrations.

1. Introduction

In our effort to understand the gas phase photochemistry and the ion chemistry of the mono-halogenated methanes, the starting step is the investigation of their vacuum UV photoabsorption spectrum. Obviously, as sufficiently proved in the past, the detailed analysis of the photoabsorption spectrum is an essential tool for the interpretation of the various spectra, e.g. the threshold photoelectron, constant ion state (CIS) spectra and ion yield in photoionization mass spectrometry.

In the frame of this work, we already examined in detail the photoabsorption spectrum of the CH_3F molecule in the 7-24 eV photon energy range [1]. In the preceding paper we went on with the photoabsorption spectrum of CH_3C1 and CD3Cl between 6-12 eV and restricted the analysis to the classification and assignment of the Rydberg series in these two molecules [2]. Numerous features have still to be interpreted in this spectrum. Essentially two previous studies mentioned and presented, partially at least, an analysis of these structures.

First, Felps et al. [3] reported the photoabsorption spectrum of CH_3X (X = Cl, Br and I) in the 61 000-69 000 cm^{-1} (7.55-8.55 eV) spectral region. They reported a splitting of about 915 cm^{-1} which was related to the spin-orbit coupling and a few vibrational modes were identified. This group [3] also examined the lowest Rydberg transitions in the same spectral region for the corresponding perdeuterated methyl halides.

The most extensive study of the vacuum UV photoabsorption spectrum of CH_3C1 has been reported by Truch et al. [4]. The spectrum was investigated in the wavelength region of 68 600-94 700 cm^{-1} (8.50-11.74 eV).

[1] Chercheur Qualifié FNRS (Belgium).

Valence-valence and Rydberg transitions were observed and assigned. The vibrational fine structure in this energy range was analyzed in some detail for the first time in this photon energy range.

The aim of this part of the present photoabsorption work is to identify and to classify the numerous features present in the vacuum UV absorption spectrum of both CH_3C1 and CD_3C1 in the 7.8-10.8 eV photon energy range. The assignment to the excitation of vibrational normal modes will be based on ab initio quantum mechanical calculations on CH_3C1^+ and CD_3C1^+ presented in this work. This will also make a detailed investigation of the isotope effect on the excited vibrational normal modes possible.

2. Experimental

2.1. Experimental setup

The experimental setup used in this work has already been described in detail elsewhere [5]. Only the most salient features will be reported here.

Synchrotron radiation available from the BESSY I facility (Berlin, Germany) is dispersed with a modified vacuum UV normal incidence 225 McPherson monochromator with a focal length of 1.5 m, instead of 1 m in the commercial version (lm-NIM-2 beamline). A laminar Zeiss grating is used for the efficient reduction of the second spectral order. It is gold coated with 1200 ℓ/mm and its transmission breaks down above 26 eV (210 000 cm^{-1} or 47 nm). The width of the entrance and exit slits of 100 μm provides a 0.1 nm resolution. The light passes through a 1 mm thick stainless steel microchannel plate necessary to ensure a differential pressure of 1:1000 before entering a 30 cm long stainless steel absorption cell. Most of the spectra are recorded without filter on the light path. However, in some instances a LiF filter is used. It can be inserted in the light beam without vacuum breakdown. This filter has a transmission cutoff at 11.8 eV (95 000 cm^{-1} or 105 nm). The vapor pressure in the cell is measured by a Balzers capacitor manometer. The light is detected by a sodium salicylate sensitized photo-multiplier located at the end of the absorption cell and in front of the monochromator exit slit. Output pulses are recorded by a 100 MHz counter. The recording of an absorption spectrum requires one scan with gas in the absorption cell and one with the empty cell. The stability of the synchrotron radiation and of the pressure in the cell ensures reliable absorption data. If required, the spectra presented in the following sections are corrected for any pressure drift. The commercially available CH_3C1, purchased from Praxair and of 99.5% purity, was used without further purification. The CD_3CL, purchased from Merck, Sharp and Dohme, is certified at 99 at.% purity. No noticeable impurity was observed by mass spectrometry at 21.2 eV photon energy. Therefore, the sample was used without further purification.

2.2. Data handling and error estimation

The wavelength calibration of the monochromator has been performed by using the Ar^+ absorption spectrum between the $^2P_{3/2}$ and the $^2P_{1/2}$ ionic states. The accuracy of this calibration was better than 2 meV. In the measurements extending from 6 to 25 eV photon energy, the photoabsorption spectrum has been recorded with an energy interval of about 10 meV. The precision on the energy position of a feature is estimated to be 15 meV. In the photoabsorption spectra extending between 6 and 12 eV photon energy, an energy increment of 1.5 meV has been adopted. The precision on the energy position of a feature is estimated to be of the order of 2 meV. Therefore, in these cases the assigned total error would be 4 meV. This evaluation is confirmed by the reproducibility of energy positions measured in four different spectra recorded in a two years interval.

3. Experimental results

3.1. The CH_3Cl photoabsorption spectrum

Fig. l(a)-(d) reproduces the photoabsorption spectrum of CH_3C1 on an expanded photon energy scale. The assignments of the observed fine structure to various vibrational progressions have been inserted in this figure. The convergence limits are the ionization energy values reported by Karlsson et al. [6] as measured by He-I photoelectron spectroscopy.

3.2. The CD_3Cl photoabsorption spectrum

The photoabsorption spectrum of CD_3C1 has been recorded between 6 and 12 eV photon energy. The fine structures, assigned to excitation of vibrational progressions in the successive Rydberg states, are clearly identified in an expanded photon energy scale, as shown in Fig. 2(a)-(d). In this case, only the first ionization

Published in: Chemical Physics (2001), vol. 272, pp. 277-292
Status: Postprint (Author's version)

limits corresponding to the two spin-orbit components, as determined in the preceding paper, are used as convergence limit for each vibronic Rydberg series.

***Fig. 1**. The vacuum UV photoabsorption spectrum of CH_3C1 on an expanded photon energy scale between 7.6 and 11.6 eV (a)-(d). The assignments are inserted by vertical bars.*

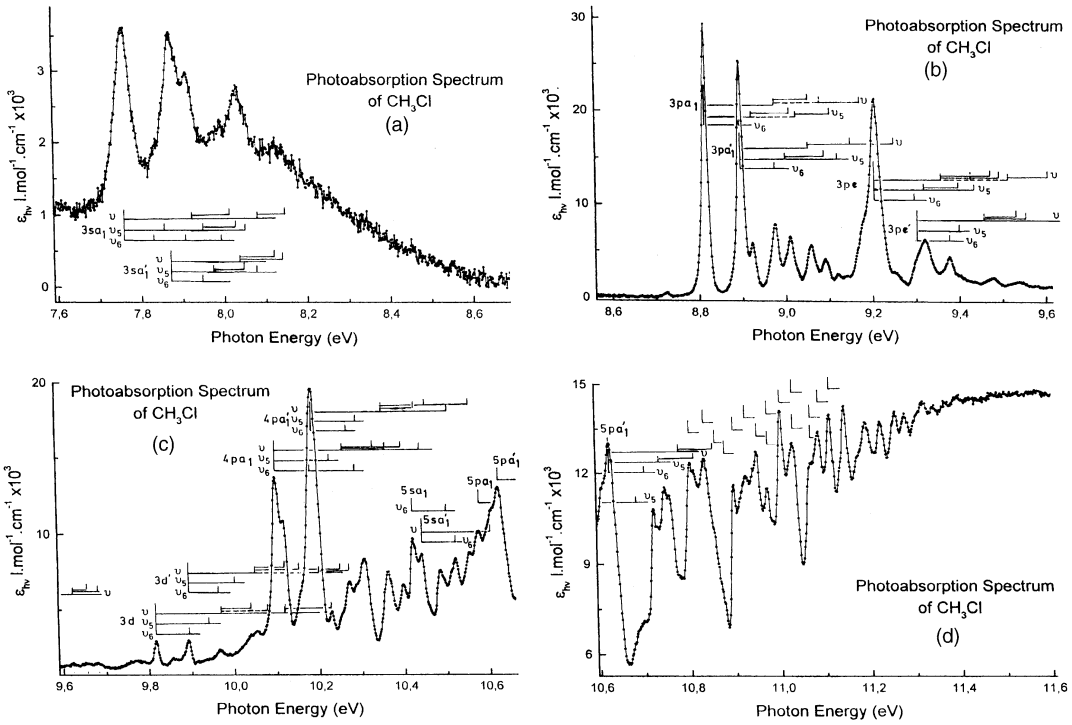

4. Ab initio calculations: procedures and results

Fairly recently, two high level ab initio quantum mechanical calculations were reported about CH3Cl and CH_3C1^+ [7, 8]. Gauld and Radom [7] used HF/6-31G and MP2 with different basis sets (6-31G, 6-311G and 6-311G**) to describe CH_3X and CH_3X^+ (X = F, Cl, OH, NH_2, SH and PH_2) and their isomeric species H_2CX^+H. They obtained the optimized geometries and thermodynamical properties. Good agreement was found between theory and experiment for most of the species, e.g. CH_3C1^+ in the C_S symmetry. Geometrical parameters of the ylidion isomer H_2CC1^+H (C_1 symmetry) were also calculated. Contrarily to the case of CH_3F^+, the ylidion H_2CC1^+H (C_1) structure is energetically less stable than the H_3CC1+ (C_S) by about 0.46 eV. In the case of CH_3F^+ the ylidion structure is more stable than H_3CF^+ by 0.065 eV. The C-Cl bond distance in the molecular ion is shortened by 0.024 A with respect to the neutral.

Lugez et al. [8] investigated the infrared spectrum of the methyl halide cations trapped in a frozen neon matrix. The discussion of their experimental results is based upon ab initio calculations at MP2 and QCISD levels. These authors reach the same conclusions concerning the relatively higher stability of the CH_3C1^+ structure. With respect to the neutral molecule, the C-Cl bond shortening upon ionization is calculated to be only 0.002 Å, instead of 0.11 Å in the case of CH_3F^+.

Furthermore, these authors [8] calculated the vibrational wave numbers in CH_3C1^+ and compared the theoretical results with their infrared data and with the values obtained for the cation by photoelectron spectroscopy [6]. However, this work was restricted to the lowest component of the Jahn-Teller split ^2E ground state of the CH_3C1^+ cation. No informations are provided about the second component. Furthermore, superimposed on this effect, and more important than in CH_3F^+, the $^2E_{3/2}$-$^2E_{1/2}$ spin-orbit splitting shows up in CH_3C1^+.

In order to obtain a complete picture of the Jahn-Teller effect in CH_3C1^+, we performed ab initio calculations on CH_3C1 and CH_3C1^+ using the GAUSSIAN94 program [9] at the MP2 level [10] with 6-31G** and 6-311G** basis sets [11,12]. The geometries are optimized respectively for the C_{3v} and the C_S symmetry

point groups. The use of MP2 level calculations with these basis sets was chosen because it is well suited, at reasonable cost, for vibrational frequency calculations [13] of neutral and ionic species. The results are shown in Table 1 for CH_3C1 ($\tilde{X}\,^1A_1$) and CH_3C1^+ ($^2A'$ and $^2A''$) together with the results provided by previous calculations [7, 8].

Fig. 2. *The vacuum UV photoabsorption spectrum of CD_3C1 on an expanded photon energy scale between 7.6 and 11.6 eV (a)-(d). The assignments are inserted by vertical bars.*

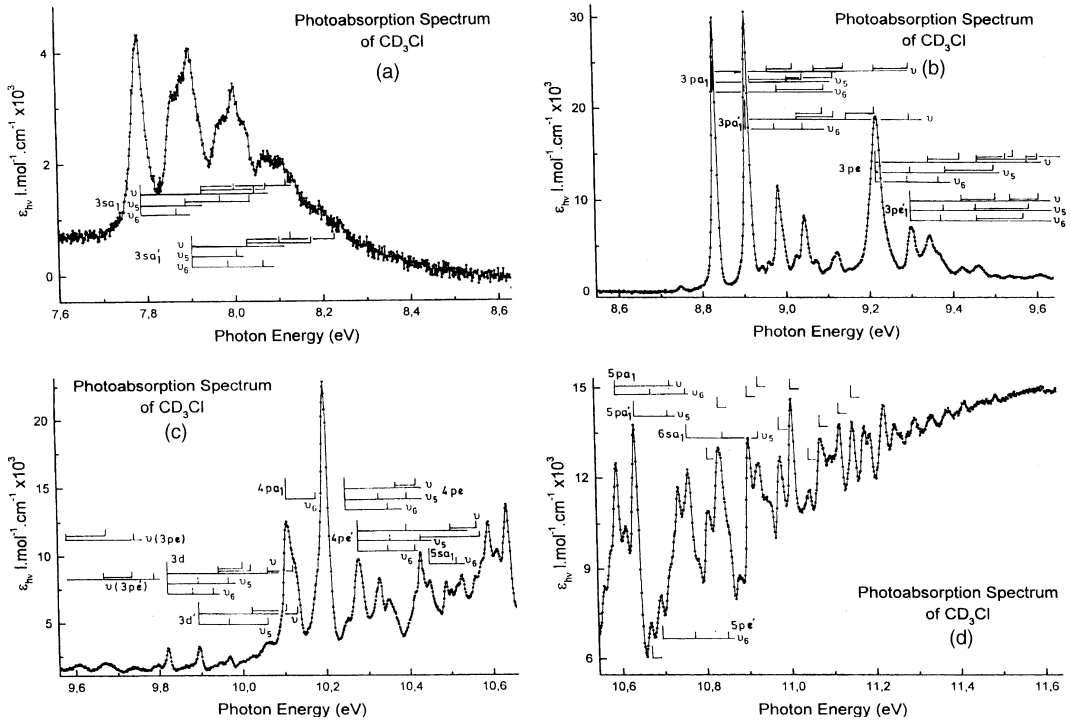

In agreement with these authors [7,8], a slight shortening of about 0.01 Å is obtained at the MP2/ 6-31G** level for the C-Cl bond after ionization in either the $^2A'$ or the $^2A''$ component of the Jahn-Teller splitting. For both the $^2A'$ and the $^2A''$ states, the largest C-H bond change involves the lengthening of the C-Hl (0.0165 Å) and C-H2 (0.0100 A) respectively (for the H atoms numbering, see figure in Table 1). Moreover the change of one valence angle (Hl-C-Cl for the $^2A'$ state or H2-C-C1 for the $^2A''$ state) and of the dihedral angle is in the 3-5° range.

The vibrational wave numbers of the neutral molecule ground state and the $^2A'$ and the $^2A''$ states of the cation have been calculated and weighted by the empirical 0.937 correction factor [13]. The results are displayed in Table 2 for CH_3C1 and CH_3C1^+ ($^2A'$ and $^2A''$) and for CD_3C1 and CD_3C1^+ in the corresponding electronic states. The nuclear motions associated with the nine normal modes are described with reference to symmetry coordinates (m_1 to m_{11}) represented in Fig. 3.

For both neutral species CH_3C1 and CD_3C1 in the $\tilde{X}\,^1A_1$ state, the present calculated and the experimental wave numbers [14,15] are in good agreement. The largest deviation is 36 cm^{-1} or 4 meV which lies within the experimental error. Concerning the $^2A'$ state of the normal and per-deuterated cation, the results provided by the present calculations satisfactorily agree with those reported by Lugez et al. [8] working at the QCISD level. The discrepancy has to be ascribed to the level difference of the compared calculations and to the use of distinct basis sets. For the $^2A''$ transition state (TS) the wave numbers obtained in this work are listed in Table 2.

Published in: Chemical Physics (2001), vol. 272, pp. 277-292
Status: Postprint (Author's version)

***Table 1** : Optimized geometries of CH_3C1 ($\tilde{X}\,^1A_1$) in the C_{3v} symmetry group and CH_3C1^+ ($^2A'$ and $^2A''$) in the C_S symmetry group calculated attheMP2/6-31G** level*

Level	C-Cl	C-Hl	C-H2	Hl-C-Cl	H2-C-C1	H2-C-C1-H1
			CH_3Cl ($X\,^1A_1$) in C_{3v} symmetry			
MP2/6-31G**	1.7759	1.0843	1.0843	108.97	108.97	120.0
[7]	1.779	1.087	1.087	108.6	108.6	120.0
[8]	1.785	-	-	-	-	-
Exptl [19]	1.776	1.085	1.085	108.6	108.6	120.0
			CH_3Cl^+ ($^2A'$) in C_S symmetry			
MP2/6-31G**	1.7671	1.1008	1.0857	103.22	108.34	116.82
MP2/6-311G**	1.7602	1.1062	1.0891	102.61	108.64	116.37
[7]	1.755	1.108	1.089	101.6	108.60	116.02
[8]	1.783	-	-	-	-	-
			CH_3Cl^+ ($^2A''$) in C_s symmetry			
MP2/6-31G**	1.7685	1.0822	1.0943	109.14	105.43	122.93

Distances are in A and angles in degrees. Comparison is made with previous calculations at their highest level [7,8] and experiment [19].

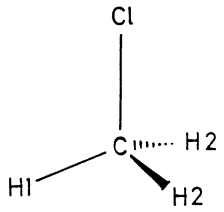

The threefold global C_{3v} symmetry of the CH3Cl system leads to three potential wells of A' symmetry on the low-energy part of the Jahn-Teller distorted potential energy surface. These minima are located at symmetrically equivalent positions corresponding to polar angles of 30°, 150° and 270° respectively. They are connected by saddle points lying at 90°, 210° and 330°. These TS belong to the A″ representation and correspond to the second state referred to in Tables 1 and 2. Fig. 4 illustrates this discussion by displaying the lower part of the Jahn-Teller distorted potential energy surface of the ^2E state of CH_3C1^+. The displayed data are provided by a second-order perturba-tional treatment [16] leading to the following equation

$$V(q_x, q_y) = V(\Delta, \phi) = E_0 - \lambda\Delta + \left[\mu - \frac{v}{2}\sin(3\phi)\right]\Delta^2,$$

Δ and φ are the polar coordinates associated with the (q_x,q_y) degenerate symmetry coordinate. The parameters λ, μ and v can be deduced from the calculated position of the potential wells along with the energies of the A' and A″ states.

When comparing the wave numbers associated with the ^{2}A' and the ^{2}A" states, the influence of the Duschinsky effect has to be mentioned [17]. As shown in Fig. 4, the normal modes resulting from a linear combination of a pair of coordinates (q_x, q_y), degenerate in the C_{3v} symmetry group, are rotated by 60° when one switches from the ^{2}A' state to the ^{2}A" state. It is therefore expected that normal modes in the C_s symmetry group correlating to degenerate modes in the C_{3v} symmetry group will be affected. This is the case for the normal modes having components on m_9, m_{10}, m_2 and m_1, i·e. for v_1 v_5, v_7, v_8 and v_9. From Table 2 it can be deduced that v_1 and v_5 are respectively 97 cm^{-1} and 135 cm^{-1} smaller in ^{2}A' than in ^{2}A". On the other hand v_7 is 179 cm^{-1} larger in ^{2}A' than in ^{2}A" and v_8 is nearly unaffected. Furthermore, v'_9 is characterized by an imaginary wave number in the ^{2}A" state and corresponds therefore to the reaction coordinate linking the three potential wells. This reaction coordinate has a strong weight on the H-pivotal coordinate m_2 which is thus the leading distortion factor associated with the Jahn-Teller effect. The symmetrical normal modes having components on m_7, m_3 and m_{11} *are* almost unaffected by going from ^{2}A' to ^{2}A". As examples, v_4 and v_6 differ by less than 12 cm^{-1}.

Published in: Chemical Physics (2001), vol. 272, pp. 277-292
Status: Postprint (Author's version)

Table 2 *: Vibrational normal modes and their corresponding wave numbers (cm^{-1}) resulting from ab initio calculations at the MP2/6-31G** level, for CH_3C1 and CD_3C1 ($\tilde{X}\,^1A_1$) and CH_3C1+ and CD_3C1+ ($^2A'$ and $^2A''$) respectively in the C_{3v} and C_S symmetry group*

Designation	Description (see Fig. 3)	Calculated wave number			
		Experimental [14,15]		This work	
		CH_3C1	CD_3C1	CH_3C1	CD_3C1
CH_3CI and CD_3CI: $\tilde{X}\,^1A_1$ in the C_{3v} symmetry					
a_1 symmetry					
vl	m_7	2967.8	2161	2969	2134
v_2	m_3	1355.0	1029	1370	1042
v_3	m_{11}	732.8	695	738	701
e symmetry					
v_4	m_{10}	3043.6	2286	3079	2293
v_5	m_2	1488.2	1058	1446	1049
v_6	m_1	1017.5	775	1013	764
		Ref. [8]		This work	
		CH_3Cl^+	CD_3Cl+	CH_3Cl+	CD_3Cl+
CH_3Cl^+ and CD_3Cl^+: $^2A'$ in the C_S symmetry					
a' symmetry					
vl	m_9	3140	2305	3014	2222
v_2	m_8	2976	2138	2844	2049
v_3	m_6	1453	1073	1395	1033
v_4	m_3	1336	979	1297	952
v_5	m_1	904	693	879	677
v_6	$m_{11} + m_4$	622	576	579	550
a" symmetry					
v_7	m_{10}	3160	2332	3023	2236
v_8	m_2	1276	906	1230	877
v_9	m_2	606	477	571	441
CH_3Cl+ and CD_3Cl^+: $^2A''$-TS in the C_S symmetry					
a' symmetry					
v'_1	m_9	-	-	3111	2319
$v'2$	m_8	-	-	2883	2077
v'_3	m_3	-	-	1386	1025
v'_4	$m_4 + m_6$	-	-	1286	936
v'_5	$m_1 + m_6$	-	-	1014	770
v'_6	m_{11}	-	-	582	563
a" symmetry					
v'_7	m_{10}	-	-	2844	2067
v'_8	m_2	-	-	1259	899
v'_9	m_2	-	-	i543	i423

The ^{2}A"corresponds to a TS. All wave numbers are corrected by the coefficient proposed by Scott and Radom [13]

Table 3 *: Gradient components ∂E/∂X, in atomic units (hartree/bohr and hartree/radian), for $^2A'$ and $^2A''$ states of CH_3Cl^+ calculated at the C_{3v} geometry of the ground state of the neutral molecule*

State	X					
	C-Cl	C-H1	C-H2	H1-C-Cl	H2-C-C1	H2-C-C1-H1
^{2}A'	-0.00670	0.00879	0.00229	-0.01640	-0.01133	-0.009464
^{2}A"(TS)	-0.00672	0.00028	0.00654	-0.00997	-0.01458	+0.009554

The calculation level is MP2/6-31G**.

On the basis of the geometrical differences between the cationic and the neutral ground states, the following vibrational motions are expected to be excited upon ionization. For the ^{2}A' state, the decrease of the H1-C-Cl angle alone (see figure in Table 1) is linked with the motion m_5 which is not represented in Table 2. However, it could be generated by a combination of v_4 or v_5 and v_6 (see Table 2 and Fig. 3). The decrease of the dihedral angle H2-C-C1-H1 is linked with the motion m_6. The increase of the bond length C-Hl alone is linked with m_8 and the decrease of C-Cl with the motion m_{11}. These symmetry coordinates are involved in the v_2, v_3 and v_6 normal modes. The latter mode and v_5 could be combined with v_4.

For the ^{2}A" state, the decrease of the H2-C-C1 angle nearly alone corresponds to the m_4 motion, the increase of H2-C-Cl-H1 is linked with m_6, the lengthening of C-H2 combined with the very small increase of C-Hl is related to m_9 and the decrease of C-Cl corresponds to m_{11}. All these nuclear symmetry coordinates correspond to the a'-type normal modes v'_1, v'_4, v'_5 and v'_6. The magnitude of the energy gradient components (see Table 3) mostly confirms this prediction with the exception of the valence angle variations. On the basis of Table 3, both the Hl-C-Cl and H2-C-C1 gradient components have about the same amplitude and the same sign for the ^{2}A' and the ^{2}A" states. For the ^{2}A' mainly the symmetry coordinate m_3 related to the v_4 mode should be active and the slight difference between the gradients could be accounted for by a properly weighted combination with m_4 or m_5. For the ^{2}A" state, the symmetry coordinate m_3 is related to the v'_3 mode and the gradient intensity for the two angles is reversed. For the dihedral angle H2-C-C1-H1 the gradients for the ^{2}A' and ^{2}A" have also about the same magnitude but opposite sign. This motion involves m_6 related to v'_4 and v'_5 in ^{2}A" and v_3 in ^{2}A'.

***Fig. 3**. Schematic representation and description of nuclear symmetry coordinates m_i, of CH_3X^+ in the C_s symmetry group.*

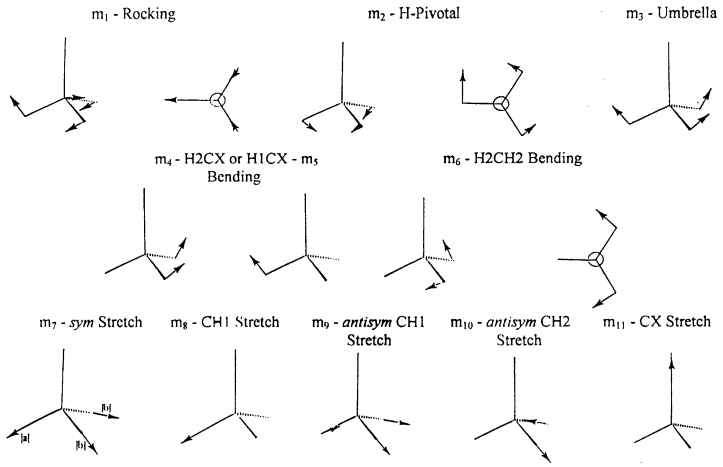

The energy gradient components are calculated at the initial geometry which corresponds to the neutral C_{3v} symmetry. At least at short times, which govern the general pattern of the photo-electron spectrum, the motion of the wave packet center will be influenced mainly by the initial gradient. The geometry of the neutral and both cationic states are not very different. The ^{2}A" TS is only 2.5 meV higher than the ^{2}A' minimum as calculated at the MP2/6-31G** level. On the other hand, the stabilization energy through the Jahn-Teller distortion is calculated to be 40 meV. It has to be compared with the value of the spin-orbit coupling in CH_3C1^+ where ΔE ($^2E_{3/2}$ — $^2E_{1/2}$) is 27 meV [6], i.e. about the same order of magnitude as the Jahn-Teller vibronic interaction. In the free Cl atom the spin-orbit splitting is 109 meV [18]. Contrarily, in CH_3F the Jahn-Teller stabilization energy was about 800 meV [1] whereas the spin-orbit splitting is negligible. The spin-orbit splitting in the free F atom is indeed 50 meV [18] and should be considerably quenched by the vibronic coupling [6].

5. Discussion of the experimental data

For clarity in the following discussion of the experimental results, the molecular orbital configuration of CH_3C1 in the C_{3v} group of symmetry has to be kept in mind, i.e.

Published in: Chemical Physics (2001), vol. 272, pp. 277-292
Status: Postprint (Author's version)

$$Cl(1s^2)C(1s^2)Cl(2s^22p^6)(1a_1)^2(2a_1)^2(1e)^4(3a_1)^2(2e)^4$$
$$: \tilde{X}\,^1A_1$$

Fig. 4. *Contour lines of the low-energy part of the Jahn-Teller distorted potential energy surface of the $CH_3C1^+(\tilde{X}^2E)$ state. The energies (eV) are given with respect to the apex (undistorted position). This diagram corresponds to a second-order perturbation treatment of the Jahn-Teller effect [16].*

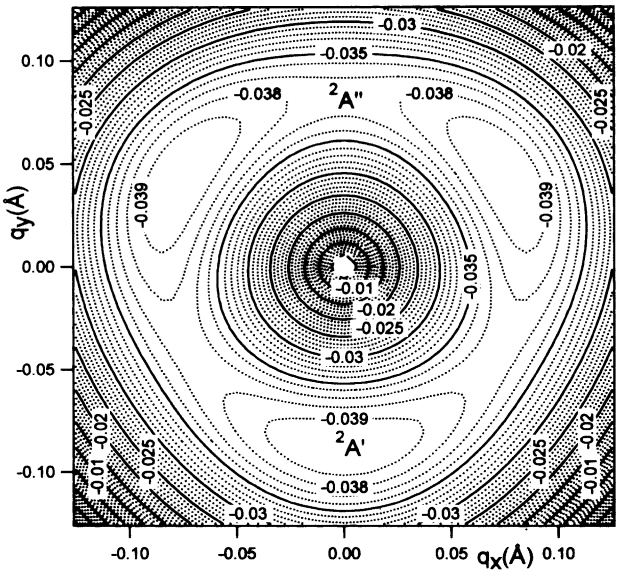

The most accurate and vibrationally well-resolved He(I) photoelectron spectrum [6] provides the adiabatic ionization energy at 11.289 ± 0.003 eV corresponding to the ground ionic state. This state shows a spin-orbit splitting of 27 ± 6 meV (218 ± 50 cm^{-1}), i.e. ionization energies measured at 11.289 ± 0.003 eV and 11.316 ± 0.003 eV [6].

General Remark: A first rough examination of the spectrum laid open two aspects. First, concerning the line shape of the vibronic structure, though dominated by sharp strong lines whose broadness is limited by the optical resolution of the monochromator, many weak or very weak lines are broad or very broad. This could be ascribed to unresolved transitions embedded in the same "line".

Secondly, the overall aspect of the absorption spectrum is made of series of short vibrational progressions with very sharp and strong lines corresponding to 0-0 transitions. Very rapidly the lines intensity becomes weak and even very weak.

This latter characteristic is closely related to the nature of the molecular orbital involved in the Rydberg excitation and, consequently, to the geometrical differences between the initial and final states.

From the ab initio calculations presented earlier (see Section 4) the main conclusion is that upon ionization, even though a Jahn-Teller distortion takes place when a $2e^{-1}$ ionization is involved, the geometrical characteristics of the CH_3C1^+ ion only slightly differ from those of the neutral molecule. This would lead to narrow vibronic "envelopes" with low vibrational excitation. The present spectral shape is in agreement with these ab initio predictions.

5.1. The $3sa_1(a'_1)$ series

As an introductory remark, the line shape of the $3sa_1(a'_1)$ series (and its associated vibrational structure) has to be pointed out. The diffuseness of these bands is considerably larger than for the higher members of this series, as well as that of the np and nd series. Particularly convincing in this respect is the comparison of the $3sa_1$ with the 3p and 3d main lines observed for CH_3C1 (see Fig. 1). The same observation holds for CD_3C1 (see Fig. 2).

Published in: Chemical Physics (2001), vol. 272, pp. 277-292
Status: Postprint (Author's version)

Table 4 *: Energies (eV), wave numbers (cm^{-1}), effective principle quantum numbers (n*), limits (eV) and assignments (0-0 means vibrationless transition) of vibrational progression of ($n\ell a_1$ or $n\ell e$) and ($n\ell a'_1$ or $n\ell e'$) Rydberg series in CH_3C1 converging respectively to the $\tilde{X}\,^2E_{3/2}$ and to $\tilde{X}\,^2E_{1/2}$ of CH_3C1^+: Panel A—$3sa_1(a'_1)$ and Panel B—np and nd (1 eV = 8065.48 cm^{-1} [20])*

	This work					Ref. [3][a]
Rydberg	**eV**	**cm^{-1}**	***n****	**Limit[b]**	**Assignment[c]**	
Panel A						
$2e \rightarrow 3sa_1$	7.759	62 582	1.936	11.289	0-0	62 540
	7.833	63 179	1.962	11.368	v_6	-
	7.858	63 380	1.960	11.399	v_5	63 455
	7.912	63 816	1.969	11.422	$2v_6$	63 745
	7.923	63 905	(1.963)[d]	(11.454)[d]	v	-
	7.992	64461	(1.963)[d]	(11.523)[d]	$3v_6$	64315
	8.014	64 639	1.963	11.545	$v+v_5$	-
	[8.032][e]	[64784][e]	1.964	11.558	$2v_5 + v_6$	64735
	[8.049][e]	[64921][e]	1.961	11.586	$3v_5$	-
	8.097	65 308	1.961	11.635	$2v$	-
	8.166	65 865	1.958	11.713	$2v + v_6$	-
$2e \rightarrow 3sa'_1$	7.873	63 501	1.987	11.316	0-0	63 455
	7.940	63 042	1.983	11.399	v_6	-
	7.975	63 324	1.987	11.422	v_5	64315
	[8.032][e]	[64784][e]	1.986	11.482	v	64735
	[8.049][e]	[64921][e]	1.984	11.506	v_5+v_6	-
	8.074	65123	(1.983)[d]	(11.524)[d]	$2v_5$	-
	8.124	65 526	1.983	11.586	$v+v_6$	65 490
	8.140	65 655	1.987	11.586	$v + v_5$	-
		-				66050
		-				66 580
		-				67 365
		-				68120
		-				68 920
						Ref. [4][a]
Panel B						
$2e \rightarrow 3pa_1$	8.815	71099	2.345	11.289	0-0	71070
	8.896	71753	2.346	11.368	v_6	71735
	8.923	71970	2.344	11.399	$v5$	71935
	8.976	72 398	2.343	[11.454]	v	72 370
	9.010	72 672	2.346	11.482	$v_5 + v_6$	72 680
	9.058	73 059	2.349	11.523	$v+v_6$	73 035
	(9.084)[d]	(73 267)[d]	(2.345)	11.558	$v + v_5$	73 285
	(9.112)[d]	(73 493)[d]	(2.345)	11.586	$2v_5 + v_6$	-
	(9.161)[d]	(73 888)[d]	(2.345)	11.635	$v + 2v_5$	-
$2e \rightarrow 3pa'_1$	8.895	71753	2.371	11.316	0-0	71753
	8.976	72 398	2.369	11.399	v_6	72 370
	9.001	72 597	2.370	11.422	v_5	-
	9.058	73 059	2.369	11.482	v	73 059
	9.090	73 325	2.373	11.506	$v_5 + v_6$	-
	9.120	73 559	2.372	11.538	$2v_5$	-
	9.138	73 702	2.371	11.558	$v+v_6$	-
	(9.166)[d]	(73 928)[d]	(2.371)	11.586	$v+v_5$	-
	9.252	74 622	2.371	11.670	$v + 2v_5$	-
$2e \rightarrow 3pe$	9.208	74269	2.557	11.289	0-0	74250
	9.298	74995	2.564	11.368	v_6	75 040

(continued on next page)

Published in: Chemical Physics (2001), vol. 272, pp. 277-292
Status: Postprint (Author's version)

Table 4 (*continued*)

	This work					Ref. [4][a]
Rydberg	**eV**	**cm^{-1}**	***n****	**Limit[b]**	**Assignment[c]**	
	9.321	75180	2.556	11.399	v_5	75210
	9.370	75 575	2.555	[11.454]	v	-
	9.403	75 842	2.558	11.482	$v_5 + v_6$	-
	9.435	76100	2.563	11.506	$2v_5$	76 395
	9.480	76463	2.559	11.558	$v + v_5$	-
	9.492	76 560	2.549	11.586	$v + 2v_6$	-
	9.606	77 479	2.561	11.681	$2v + v_6$	-
2e → 3pe'	9.298	74995	2.597	11.316	0-0	75 040
	9.378	75 640	2.595	11.399	v_6	75 700
	9.403	75 842	2.595	11.422	v_5	-
	9.538	76931	2.595	11.558	$v + v_6$	76915
	9.576	77 237	2.601	11.586	$v + v_5$	-
	9.622	77 608	2.599	11.635	$2v$	-
	9.654	77 866	2.597	11.67	$v + 2v_5$	-
	9.679	78 068	2.586	11.713	$2v + v_6$	-
Not	9.703	78 262			x	-
classified	9.769	78 794			y	-
	9.856	79 496			$x + 0.155$	-
	9.879	79 681			$y + 0.110$	-
2e→3d	9.816	79173	3.040	11.298	0-0	79170
	9.892	79 786	3.036	11.362	$v6$	-
	9.934	80125	3.047	11.399	v_5	-
	10.040	80980	3.046	11.506	$v + v_6$	81000
	[10.088]	81367	3.040	[11.558]	$v + v_5$	-
	10.119	81617	3.045	11.586	$v + 2v_6$	81645
	10.230	82 512	[3.062]	11.681	$2v + v_5$	-
2e → 3d'	9.892	79 786	3.092	11.316	0-0	79 800
	9.964	80 399	3.079	11.399	$v6$	80400
	10.002	80 673	3.095	11.422	v_5	81000
	10.054	81093	3.086	11.482	v	81130
	10.119	81617	3.092	11.542	$v + v_6$	81645
	10.158	81932	3.086	11.586	$v + v_5$	-
	10.254	82706	3.088	11.681	$v + 2v_5$	82 875
	10.290	82996	3.092	11.713	$2v + v_6$	83015
2e → 4pa$_1$	10.102	81180	3.386	11.289	0-0	81130
	[10.182]	82125	3.387	11.368	v_6	-
	10.230	82 512	3.378	11.422	v_5(?)	82 520
	10.290	82996	3.378	11.482	$2v_6$	83015
	10.308	83 142	3.370	11.506	$2v_5$	83 175
	10.363	83 585	3.374	11.558	$v + v_5$	83 625
	[10.398]	83 875	[3.384]	11.586	$v + 2v_6$	83 920
	[10.448]	84271	[3.386]	11.635	$2v$ or $v + 2v_5$	84275
	10.486	84 577	[3.390]	11.67	$2v + v_6$	-
2e → 4pa'$_1$	10.193	82190	3.476	11.316	0-0	82275
	10.273	82 851	3.476	11.399	v_6	82 875

(continued on next page)

Table 4 (*continued*)

	This work					Ref. [4][a]
Rydberg	**eV**	**cm^{-1}**	***n****	**Limit[b]**	**Assignment[c]**	
	10.290	82996	3.467	11.422	v_5	83015
	[10.354]	83 512	3.473	11.482	v	-
	10.426	84093	3.467	11.558	$v + v_6$	84095
	10.459	84 359	3.474	11.586	$v+v_5$	-
	10.515	84811	3.485	11.635	$2v$	-
	10.555	85135	3.476	11.681	$v + 2v_5$	85195
2e → 5sa$_1$	10.422	84061	3.961	11.289	0-0	84095
	[10.501]	[84 698]	[3.961]	11.368	v_6	84 625
2e → 5sa'$_1$	10.441	84214	3.943	11.316	0-0	84275
	10.522	84 868	3.939	11.399	v_6	84935
	10.609	85 569	3.948	11.482	v	-
2e → 5pa$_1$	10.578	85 319	4.375	11.289	0-0	85 340
	10.684	86174	4.362	11.399	v_5	86190
2e → 5pa'$_1$	10.624	85 690	4.434	11.316	0-0	85 780
	10.696	86271	4.399	11.399	v_6	-
	[10.780]	[86948]	4.402	11.482	v	87 025
	10.810	87190	4.421	11.506	$v_5 + v_6$	87175
	10.867	87 650	4.437	11.558	$v + v_6$	87 720
Not	10.756	86755				86775
classified	10.912	88013				88 030
	10.941	88 247				88 235
	11.121	89 699				89 695
	11.134	89 804				-

[a]Data of Refs. [3,4] reproduced without assignment.
[b] From Ref. [6].
[c]The normal mode v stays for v_3 or v_4: for details see text.
[d]Data in brackets: calculated convergence limits using the indicated n* values.
[e]Data in square brackets: ambiguous assignment.

Furthermore, the intensity of the first member of the $n$sa$_1$(a'$_1$) transitions is relatively low. The vibrational structure associated with the higher members of this series will very likely be burried under the more intense np and nd series, particularly when the n^{-3} intensity law is kept in mind. However, the two spin-orbit components of the 3s-member are fairly well isolated and lead therefore to well-separated vibrational progressions. However, the smallness of the spin-orbit splitting will make some overlap unavoidable.

The features pertaining to the 3s-series will be discussed separately and their energy positions are listed in Tables 4 (Panel A) and 5 (Panel A) for CH_3C1 and CD_3C1 respectively.

From the data obtained in the present work for CH_3C1, and the ionization limits measured by high resolution He(I) photoelectron spectroscopy [6], a vibrational assignment has been possible for both the 3sa$_1$ and the 3sa'$_1$ components. For both progressions, the features are characterized by a fairly constant effective principal quantum number, i.e. $n_{3/2}$* = 1-962 ± 0.003 for the 3sa$_1$ and $n_{1/2}$* = 1-985 ± 0.002 for the 3sa'$_1$. From the present analysis three vibrational normal modes appear to be active upon excitation. On the basis of our calculation these are identified as being v_6, v_5 and v modes. Averaging over the the energy intervals available from the two spin-orbit components of the 2e → 3s transitions observed in this energy range, values of $hc\omega_6$ = 75 ± 3 meV (605 ± 20 cm^{-1}), $hc\omega_5$ = 99 ± 3 meV (798 ± 20 cm^{-1}) and $hc\omega$ = 164 ± 3 meV (1323 ± 20 cm^{-1}) are obtained. These three values have to be compared with the predicted wave numbers (see Table 2) of ω_6 = 579 cm^{-1}, ω_5 = 879 cm^{-1} and ω_4 = 1297 cm^{-1} or ω_3 = 1395 cm^{-1}. From the discussion in Section 4 some arguments favor v_3 as being the most likely. However, the confidence of these wave numbers could perhaps be improved by the analysis of the vibrational structure observed at higher energies. It has to be pointed out that the error mentioned above is the largest deviation from the mean interval for about 12 observations only. The present results can only be

compared with the data reported by Felps et al. [3]. From Table 4 (Panel A) an agreement within about 100 cm^{-1}, or better, is found between the two experiments. A better signal/noise ratio in the earlier work allowed the authors to observe the vibrational structure at higher energies (see Table 4 (Panel A)). The assignments are difficult to compare, Felps et al. [3] limiting their discussion to the framework of the C_{3v} symmetry of the neutral ground state of CH_3C1. They explicitly mention wave numbers of 655, 915 and 1205 cm^{-1}. However, the authors express "several reasons to doubt on the correctness of the above assignments".

Table 5 *: Energies (eV), wave numbers (cm^{-1}) and assignments (0-0 means vibrationless transition) of vibrational progressions of ($n\ell a_1$ or $n\ell e$) and ($n\ell a'_1$ or $n\ell e'$) Rydberg series in CD_3Cl converging respectively to the $\tilde{X}\,^2E_{3/2}$ and $\tilde{X}\,^2E_{1/2}$ of CD_3Cl^+: Panel A—$3sa_1(a'_1)$ and Panel B—np and nd (1 eV = 8 065.48 cm^{-1} [20])*

This work				Felps et al. [3]
Rydberg	**eV**	**cm^{-1}**	**Assignment**	
Panel A				
$2e \rightarrow 3sa_1$	7.789	62 824	0-0	62 835
	7.863	63 420	v_6	63 490
	7.882	63 574	v_5	63 655
	7.922	63 905	v	63 840
	7.966	64251	$v_5 + v_6$	64 370
	8.026	64752	$v + v_6$	64765
	8.035	[64 808]	$2v_6 + v_5$	-
	[8.046][a]	[64 897]	$[2v]$	-
	8.074	65 090	$v + 2v_6$	65190
	[8.131][a]	65 582	$v + 2v_5$	65 640
$2e \rightarrow 3sa'_1$	7.903	63 743	0-0	63 785
	7.980	64 365	v_6	64 370
	8.002	64 542	v_5	64 560
	-	-	-	64 635
	8.028	64752	v	64765
	[8.046][a]	[64 897]	$2v_6$	64 890
	8.104	65 389	$v + v_6$	65 425
	[8.131][a]	65 582	$v + v_5$	64 640
	8.196	66107	$v + 2v_6$	-
	8.241	66470	$v + 2v_5$	-
Panel B				
$2e \rightarrow 3pa_1$	8.833	71244	0-0	
	8.960	72269	v	
	8.983	72454	$2v_6$	
	9.025	72793	$v + v_6$	
	9.045	72954	$v + v_5$	
	9.072	73 172	$2v$	
	9.097	73 374	$v + 2v_6$	
	9.112	73 495	$[v + v_5 + v_6]$	
	9.123	73 584	$v + 2v_5$	
	9.153	73 825	$2v + v_6$	
	9.222	74 382	$3v$	
	9.301	75 019	$3v + v_5$	
$2e \rightarrow 3pa'_1$	8.909	71866	0-0	
	8.976	72 398	v_6	
	9.045	72954	$2v_6$	
	9.097	73 172	$v + v_6$	
	9.123	73 584	$v + v_5$	
	9.153	73 825	$2v$	
	9.222	74 382	$2v + v_6$	
	9.301	75 019	$3v$	
$2e \rightarrow 3pe$	9.222	74 382	0-0	
	9.301	75 019	v_5	

(continued on next page)

Published in: Chemical Physics (2001), vol. 272, pp. 277-292
Status: Postprint (Author's version)

Table 5 (*continued*)

Rydberg	eV	cm^{-1}	Assignment
	9.346	75 382	ν
	9.370	75 576	$2\nu_6$
	9.421	75 987	$\nu + \nu_6$
	9.462	76318	2ν
	9.502	76 640	$\nu + 2\nu_5$
	9.535	76907	$2\nu + \nu_6$
	9.556	77 076	$2\nu + \nu_5$
	9.583	77 286	3ν
	9.607	77 487	$2\nu + 2\nu_6$
	9.682	78 092	$3\nu + \nu_5$
	9.739	78 552	4ν
2e → 3pe'	9.301	74 382	0-0
	9.370	75 576	ν_6
	9.421	75 987	ν
	9.462	76318	$2\nu_6$
	9.502	76 640	$\nu + \nu_5$
	9.535	76907	2ν
	9.556	77 076	$\nu + 2\nu_6$
	9.583	77 286	$\nu + 2\nu_5$
	9.607	77 487	$2\nu + \nu_6$
	9.670	77 996	3ν
	9.739	78 552	$3\nu + \nu_6$
	9.796	79 012	4ν
2e → 3d	9.820	79 205	0-0
	9.931	80101	$2\nu_6$
	9.946	80222	ν
	9.969	80407	$2\nu_5$
	10.002	80 603	$\nu + \nu_6$
	10.026	80 867	$\nu + \nu 5$
	10.063	81165	2ν
	10.110	81544	$\nu + 2\nu_5$
	10.126	81673	$2\nu + \nu_6$
2e → 3d'	9.895	79 810	0-0
	9.969	80407	ν_5
	10.026	80 867	ν
	10.063	81165	$2\nu_5$
	10.110	81544	$\nu + \nu_5$
	10.126	81 673	2ν
2e → $4pa_1$	10.110	81544	0-0
	10.178	82093	ν_6
	10.208-10.279	82278	Lyman α + unidentif.
2e → 4pe	[10.239]	82 585	0-0
	10.329	83311	ν_5
	10.351	83 488	$2\nu_6$
	10.372	83 658	ν
	10.399	83 875	$2\nu_5$
	10.428	84109	$\nu + \nu_6$
2e → 4pe'	10.280	82916	0-0
	10.351	83 488	ν_6

(continued on next page)

Table 5 (*continued*)

Rydberg	eV	cm^{-1}	Assignment
	10.399	83 875	ν
	10.410	83 964	$2\nu_6$
	10.428	84109	$2\nu_5$
Miscellaneous	10.501	84 698	$4pa'_1 + 2\nu$
	10.515	84811	$5sa_1 + \nu_6$
	10.560	85174	$4pa'_1 + 2\nu + \nu_6$
	10.575	85 295	$4pa'_1 + \nu + 2\nu_5$
	10.612	85 593	$4pa'_1 + 2\nu + \nu_5$ or $4d' + \nu_5$
	10.716	86432	$4d' + \nu + \nu_5$ or $5pe + \nu/5pe' + \nu_5$
	10.737	86 601	$4d' + \nu + \nu_5$ or $5pe + 2\nu_6$
	10.857	87 569	$5d + \nu 5$ or $5pa'_1 + 2\nu_6$
	10.929	88150	$5d'(6sa'_1) + \nu/5d + \nu_5 + \nu_6/6sa_1 + \mathbf{2\nu_5}$
	10.959	88 392	$6pe'(6pa_1) + \nu_5/6pe + \nu/5d'(6sa'_1) + \mathbf{2\nu_5}$

[a]Data in brackets: ambiguous assignments.

The energy positions recorded for the corresponding Rydberg transitions in CD_3C1 are listed in Table 5 (Panel A), as well as tentative assignments. From these observations the normal modes and the corresponding averaged wave numbers are $hc\omega_6 = 72 \pm 7$ meV (580 ± 50) cm^{-1}, $hc\omega_5 = 100 \pm 4$ meV (806 ± 30 cm^{-1}) and $hc\omega = 128 \pm 4$ meV (1032 ± 30 cm^{-1}). The predicted wave numbers are $\omega_6 = 550$ cm^{-1} and $\omega_5 = 677$ cm^{-1}. For the third mode $\omega_4 = 952$ cm^{-1} and $\omega_3 = 1033$ cm^{-1} could be used for comparison. The ratios, as defined by $\rho = (\omega_H/\omega_D)_i$, based on the ab initio calculated wave numbers are $\rho_3 = 1.350$, $\rho_4 = 1.363$, $\rho_5 = 1.298$ and $\rho_6 = 1.053$. The same ratios obtained from experiment are $\rho = 1.28 \pm 0.06$, $\rho_5 = 0.99 \pm 0.06$ and $\rho_6 = 1.04 \pm 0.16$. The largest discrepancy is noticed for ρ_5. In the present case also a further analysis could improve the first values based on the examination of only one transition. It could also be helpful to decide whether ν_3 or ν_4 is involved in this spectrum. Theoretical considerations (see Section 4) argue in favor of the ν_3 normal mode. However, the excitation of the unidentified ν normal mode up to $\nu = 4$ (see Table 5 (Panel B)) would suggest that it is Jahn-Teller non-active. This would favor its assignment to ν_4 (the CH_3-umbrella mode).

5.2. The $nsa_1(a'_1)$, $npa_1(a'_1)$, npe(e') and nd(d') series ($n > 3$)

Table 4 (Panel B) shows a classification and assignments of the fine structure above the 8.8 eV photon energy. The results of the present work can only be compared with the earlier results reported by Truch et al. [4]. As can be seen from Table 4 (Panel B), comparing the columns 3 and 7, a better agreement is found with these experimental results: the discrepancy is of about 50 cm^{-1} (about 6 meV), randomly distributed.

Based on the known convergence limits resulting from photoelectron spectroscopy experiments [6] effective principal quantum numbers have been allocated to each vibronic transition. These have been determined earlier for the 0-0 Rydberg transitions [2]. As shown in Table 4 (Panel B), column 4, the calculated effective principal quantum numbers using these data are nearly constant over one state. The variations are mostly of the order of a few thousandth. This parameter has been demonstrated to be sensitive enough to be used as one argument to ascribe the feature as pertaining to one vibrational progression of the same Rydberg transition [1]. Most of the lines have been assigned by this method. Just a few lines could not be classified (see end of Table 4 (Panel B)).

With the help of this hypothesis, one observes the excitation of only three vibrational modes as defined

in Section 4, i.e. ν, ν_5 and ν_6. The ν_5 and ν_6 modes involve respectively the (CH_3 rocking + C-Cl stretching) and the CH_3 bending motions. The ν_4 mode corresponds to the symmetric, Jahn-Teller inactive, CH_3-umbrella mode, whereas the ν_3 mode is described by the antisymmetric H2CH2 bending motion. Averaging over all the values available from the present observations listed in Table 4 (Panel B), values of $hc\omega_6$ = 77 ± 7 meV (621 ± 60 cm^{-1}), $hc\omega_5$ = 104 ± 7 meV (839 ± 60 cm^{-1}) and $hc\omega$ = 162 ± 3 meV (1307 ± 20 cm^{-1}). These values are in fairly good agreement with those deduced from the data listed in Table 4 (Panel A). Though being in the error limits the wave number associated to ν_5 is slightly larger, i.e. 104 meV (839 cm^{-1}) instead of 99 meV. The present value is closer to the ab initio predicted 879 cm^{-1}. Formally, the assignment of the $hc\omega$ = 162 meV to ν_3 or ν_4 remains open.

Table 5 (Panel B) displays the energy positions and assignments of the structures observed in CD_3C1. At the end of Table 5 (Panel B) we gathered the isolated peaks observed above 10.5 eV photon energy and not assigned to 0-0 Rydberg transitions. Tentative assignments, with several reasonable but not all combinations, are reported in column 4.

Assignments were attempted and essentially based on the invariability of energy intervals between lines, within about 5-10 meV (i.e. about twice the error limit). On the basis of the observed intensities and the strong variations of the line width many structures were assigned to different excitations. The values of the wave numbers deduced from all the direct observations and their combinations are averaged for the three observed vibrational excitations. The average over 30-60 observations leads to values of $hc\omega_6$ = 66 ± 5 meV (532 ± 40 cm^{-1}), $hc\omega_5$ = 81 ± 4 meV (653 ± 30 cm^{-1}) and $hc\omega$ = 124 ± 4 meV (1000 ±30 cm^{-1}). Compared to the values determined from the 2e → 3s transitions (see Table 4) all three wave numbers are corrected downwards, particularly the $hc\omega_5$ which was estimated at 99 meV. The comparison with the ab initio calculated values is fairly good, i.e. ω_6 = 550 cm^{-1}, ω_5 = 677 cm^{-1} whereas ω_3 = 1033 cm^{-1} and ω_4 = 952 cm^{-1}. A stronger argument favoring the present values is the isotope shift measured by the ratio ρ. As mentioned earlier its value was 0.99 ± 0.06 instead of 1.298 predicted by ab initio calculations. Con-trarily, the new ratio value of ρ_5 = 1.28 ± 0.15 compares fairly well with that predicted value. The two other experimental isotopic ratios ρ_6 = 1.17 ± 0.13 and ρ = 1.31 ± 0.07 have to be compared with the theoretical values (see Section 4) of ρ_6 = 1.053 and ρ_3 = 1.350 and ρ_4 = 1.362. From the present analysis, comparing the experimental values, with their respective errors, and the calculated values of ω_3 and ω_4, it is difficult to make an unambiguous assignment to the wave number of 1000 ± 30 cm^{-1}.

6. Conclusions

After the analysis of the vacuum UV spectrum of CH_3C1 and CD_3C1 in terms of Rydberg series (see preceeding paper part I), the observed abundant fine structure has been investigated in the present contribution. It has been analyzed in terms of short vibrational progressions. To help in their assignment, for both molecules the geometry and the vibrational wave numbers of all normal modes of the neutral molecule and the cation ground electronic states were calculated by ab initio quantum mechanical methods. The Jahn-Teller distortion upon ionization has also been considered and calculated. The fairly good agreement between experimental and predicted wave numbers, as well as the isotope effect, allowed us to assign the observed progressions to three vibrational modes. Two of them can be identified unambiguously as ν_5 (ω_5 = 653 ± 30 cm^{-1}) (CH_3 rocking + C-Cl stretching) and ν_6 (ω_6 = 532 ± 40 cm^{-1}) (CH_3 bending). The assignment of the third vibration with ω = 1000 ± 30 cm^{-1} to ν_3 (predicted at 1033 cm^{-1}) or ν_4 (predicted at 952 cm^{-1}) remains doubtful owing to the lack of experimental precision. Some arguments would favor the ν_4 CH_3-umbrella mode excitation.

Acknowledgements

We are indebted to the University of Liège, the Freie Universität Berlin and the Bundesminis-te-rium für Forschung und Technologie for financial support. H.B. acknowledges the Fonds der Chem-ischen Industrie for financial support. R.L., B.L. and A.H. gratefully acknowledge the European Community for its support through its TMR programme (Contract EU-TMR-ERBFMGE-CT-970123). B.L. thanks the Fonds National de la Recherche Scientifique (Belgium) for a research associate position. This work has also been supported by the Direction de la Recherche Scientifique de la Communauté Française de Belgique through an Action de Recherche Concertée (ARC). D.D.'s contribution was supported by the Belgian Programme of Pôles d'Attraction Inter-universitaires (PAI no. P4/03) initiated by the Belgian state, the Prime Minister's Office, the Federal Office of Scientific, Technical and Cultural Affaires. We gratefully acknowledge the referees for their critical reading of the manuscript and the relevance of their suggestions. We also wish to thank the BESSY I staff for the outstanding maintenance of the equipment.

Published in: Chemical Physics (2001), vol. 272, pp. 277-292
Status: Postprint (Author's version)

References

[1] R. Locht, B. Leyh, A. Hoxha, D. Dehareng, H.W. Jochims, H. Baumgartel, Chem. Phys. 257 (2000) 283.

[2] R. Locht, B. Leyh, A. Hoxha, H.W. Jochims, H. Baumgärtel, Chem. Phys. 272 (2001) 259.

[3] S. Felps, P. Hochmann, P. Brint, S.P. McGlynn, J. Mol. Spectrosc. 59 (1976) 355.

[4] D.T. Truch, D.R. Salomon, D.A. Armstrong, J. Mol. Spectrosc. 78(1979)31.

[5] A. Hoxha, R. Locht, B. Leyh, K. Hottmann, H.W. Jochims, H. Baumgärtel, Chem. Phys. 260 (2000) 237.

[6] L. Karlsson, R. Jadrny, L. Mattsson, F.T. Chau, K. Siegbahn, Phys. Scripta 16 (1977) 225.

[7] J.W. Gauld, L. Radom, J. Phys. Chem. 98 (1994) 777.

[8] C.L. Lugez, D. Forney, M.E. Jacox, K.K. Ikura, J. Chem. Phys. 106 (1997) 489.

[9] M.J. Frisch, G.W. Trucks, H.B. Schlegel, P.M.W. Gill, B.G. Johnson, M.A. Robb, J.R. Cheeseman, T.A. Keith, G.A. Petersson, J.A. Montgomery, K. Raghavachari, M.A. Al-Laham, V.G. Zakrzewski, J.V. Ortiz, J.B. Fores-man, J. Ciolowski, B.B. Stefanow, A. Nanayakkara, M. Challocombe, C.Y. Peng, P.Y. Ayala, W. Chen, M.W. Wong, J.L. Andres, E.S. Replogle, R. Gomperts, R.L. Martin, D.J. Fox, J.S. Binkley, D.J. Defrees, J. Baker, J.P. Stewart, M. Head-Gordon, C. Gonzalez, J.A. Pople, GAUSSIAN94 (Revision D.4), Gaussian Inc, Pittsburgh, PA, 1996.

[10] [a] MP2 = second order Møller-Plesset perturbation framework: C. Moller, M.S. Plesset, Phys. Rev. 46 (1934) 618; [b] R. Krishnan, J.A. Pople, Int. J. Quant. Chem. 14 (1978) 91.

[11] W.J. Hehre, R. Ditchfield, J.A. Pople, J. Chem. Phys. 56 (1972) 2257.

[12] T. Clark, J. Chandrasekhar, G.W. Spitznagel, P.V.R. Schleyer, J. Comp. Chem. 4 (1983) 294.

[13] A.P. Scott, L. Radom, J. Phys. Chem. 100 (1996) 16502.

[14] G. Herzberg, Molecular Spectra and Molecular Structure. III. Electronic Spectra and Electronic Structure of Polyatomic Molecules, D. Van Nostrand Company, Princeton, NJ, 1967.

[15] G. Herzberg, Molecular Spectra and Molecular Structure. II. Infrared and Raman Spectra of Polyatomic Molecules, D. Van Nostrand Company, New York, 1945.

[16] R.L. Martin, E.R. Davidson, Mol. Phys. 35 (1978) 1713.

[17] F. Duschinsky, Acta Physicochimica URSS 7 (1937) 551.

[18] C.E. Moore, Atomic Energy Levels, vol. I, circ. 467, US Department of Commerce, N.B.S. Washington DC, 1949.

[19] P. Jensen, S. Brodersen, G. Guelachvili, J. Mol. Spectrosc. 88 (1981) 378.

[20] E.R. Cohen, B.N. Taylor, J. Phys. Chem. Ref. Data 37 (1973) 663.